Electrochemical Intercalation of Oxygen in Nd_2NiO_{4+x} ($0 \leq x \leq 0.18$) at 298 K

S. Bhavaraju, J. F. DiCarlo, D. P. Scarfe, I. Yazdi, and A. J. Jacobson*

Department of Chemistry and Texas Center for Superconductivity, University of Houston, Houston, Texas 77204-5641

Received July 6, 1994. Revised Manuscript Received August 25, 1994®

Electrochemical intercalation of oxygen into Nd_2NiO_{4+x} has been investigated by potential step experiments (5 mV steps, 10 μA cutoff current) in aqueous 1 M KOH at 298 K. Stoichiometric Nd_2NiO_4 is obtained on the initial reduction of the starting material $Nd_2NiO_{4.18}$. On reoxidation, a maximum composition of $Nd_2NiO_{4.1}$ is obtained below the potential where oxygen evolution is observed. In the composition range $0.0 \leq x \leq 0.08$ intercalation is reversible. The electrochemical data show two-phase behavior in the composition range $0.01 \leq x \leq 0.04$ and a single-phase region $0.04 \leq x \leq 0.08$. Parallel X-ray diffraction studies show that Nd_2NiO_{4+x} is orthorhombic for $0 \leq x \leq 0.01$, tetragonal for $0.04 \leq x \leq 0.08$ and orthorhombic at $Nd_2NiO_{4.18}$. An enthalpy of oxidation of -204 kJ/mol of O_2 was obtained from the electrochemical data in the single-phase region.

Introduction

Several reports have shown that oxygen can be electrochemically intercalated into oxides with the perovskite and perovskite related structures at 298 K.[1-12] Many studies have focused on La_2CuO_4, which on electrochemical intercalation becomes superconducting with a transition temperature of ~45 K. Our electrochemical results on La_2CuO_{4+x} have shown that oxygen intercalation is quantitative in the sense that all the oxygen atoms which are intercalated on oxidation can be removed on reduction.[10] The voltage composition profiles on oxidation and reduction, however, are very different, even at low current densities, and equilibrium is difficult to achieve. Phase separation as a function of both excess oxygen and temperature has been observed in both electrochemical and structural studies.[13-15]

In contrast, electrochemical studies on La_2NiO_{4+x} ($0 \leq x \leq 0.145$) have shown that oxygen intercalation and deintercalation (oxidation–reduction) is reversible at 298 K.[8,17] Consistent with this observation, the phase diagram obtained from electrochemical measurements on La_2NiO_{4+x} at 298 K is in excellent agreement with the phase diagram obtained on single-crystal samples equilibrated at higher temperatures.[18] The enthalpy of oxidation determined from the room-temperature electrochemical data for La_2NiO_{4+x} is in agreement with the corresponding value obtained by calorimetric methods.[19] The phase diagram of La_2NiO_{4+x} becomes more complex below ambient temperature due to additional phase separation.[16,17]

Pr_2NiO_4 and Nd_2NiO_4 are both isostructural with La_2NiO_4.[20-22] As the size of the rare-earth ion decreases, the structural distortions from the ideal tetragonal K_2NiF_4 structure become more pronounced. For example, all of the stoichiometric phases are orthorhombic (space group *Bmab*) but the distortion, as measured by the orthorhombic strain $(b - a)/(b + a)$, increases from 0.0065 in La_2NiO_4 to 0.0158 and 0.0183 in Pr_2NiO_4 and Nd_2NiO_4, respectively.[18,23] Maximum oxygen contents of 4.168,[18] 4.215,[23] and 4.16[24] for La, Pr, and Nd, respectively, are obtained on oxidation in oxygen. The degree of distortion in the oxidized phases is reduced for all three systems.

The structural distortions in Nd_2NiO_4 are a function of both oxygen stoichiometry and temperature and are known to influence the transport and magnetic properties.[24-32] Electrical conductivity measurements on

® Abstract published in *Advance ACS Abstracts,* October 1, 1994.

(1) Kudo, T.; Obayashi, H.; Gejo, T. *J. Electrochem. Soc.* **1975**, *122*, 159.
(2) Wattiaux, A.; Park, J.-C.; Grenier, J.-C.; Pouchard, M. *C. R. Acad. Sci. Paris* **1990**, *310*, 1047.
(3) Wattiaux, A.; Fournès, L.; Demourgues, A.; Bernaben, N.; Grenier, J.-C.; Pouchard, M. *Solid State Commun.* **1991**, *77*, 489.
(4) Rudolf, P.; Paulus, W.; Schöllhorn, R. *Adv. Mater.* **1991**, *3*, 438.
(5) Grenier, J.-C.; Wattiaux, A.; Doumerc, J. P.; Dordor, P.; Fournès, L.; Chaminade, J.; Pouchard, M. *J. Solid State Chem.* **1992**, *96*, 20.
(6) Grenier, J.-C.; Wattiaux, A.; Demourgues, A.; Pouchard, M.; Hagenmuller, P. *Solid State Ionics* **1993**, *63–65*, 825.
(7) Bezdicka, P.; Grenier, J.-C.; Wattiaux, A.; Pouchard, M.; Hagenmuller, P. *Z. Anorg. Allg. Chem.* **1993**, *619*, 7.
(8) Demourgues, A.; Wattiaux, A.; Grenier, J.-C.; Pouchard, M.; Soubeyroux, J. L.; Dance J. M.; Hagenmuller, P. *J. Solid State Chem.* **1993**, *105*, 458.
(9) DiCarlo, J. F.; Yazdi, I.; Bhavaraju, S.; Jacobson, A. J. *Chem. Mater.* **1993**, *5*, 1692.
(10) Bhavaraju, S.; DiCarlo, J. F.; Yazdi, I.; Jacobson, A. J.; Feng, H. H.; Li, Z. G.; Hor, P.-H. *Mater. Res. Bull.* **1994**, *29*, 735.
(11) Chou, F. C.; Cho, J. H.; Johnston, D. C. *Physica C* **1992**, *197*, 303.
(12) Scolnik, J.; Rappaport, M.; Hass, N.; Dai, U.; Cahen, D. *Physica C* **1993**, *209*, 1993.
(13) Jorgensen, J. D.; Dabrowski, B.; Pei, S.; Richards, D. R.; Hinks, D. G. *Phys. Rev. B* **1989**, *40*, 2187.
(14) Demourgues, A.; Weill, F.; Grenier, J.-C.; Wattiaux, A.; Pouchard, M. *Physica C* **1992**, *192*, 425.
(15) Radaelli, P. G.; Jorgensen, J. D.; Kleb, R.; Hunter, B. A.; Chou, F. C.; Johnston, D. C. *Phys. Rev. B* **1994**, *49*, 6239.
(16) Tranquada, J. M.; Kong, Y.; Lorenzo, J. E.; Buttrey, D. J.; Rice, D. E.; Sachan, V. *Phys. Rev. B*, in press.
(17) Yazdi, I.; Bhavaraju, S.; DiCarlo, J. F.; Scarfe, D. P.; Jacobson, A. J. *Chem. Mater.*, to be published.
(18) Rice, D. E.; Buttrey, D. J. *J. Solid State Chem.* **1993**, *105*, 197.
(19) DiCarlo, J. F.; Mehta, A.; Banschick, D.; Navrotsky, A. *J. Solid State Chem.* **1993**, *103*, 186.
(20) Rabenau, A.; Eckerlin, P. *Acta Crystallogr.* **1958**, *11*, 304.
(21) Willer, B.; Daire, M. C. *C. R. Acad. Sci. Paris* **1968**, *267*, 1482.
(22) Lehmann, U.; Müller-Buschbaum, Hk. *Z. Naturforsch.* **1980**, *35b*, 389.
(23) Sullivan, J. D.; Buttrey, D. J.; Cox, D. E.; Hriljac, J. *J. Solid State Chem.* **1991**, *94*, 337.
(24) Arbuckle, B. W.; Ramanujachary, K. V.; Zhang, Z.; Greenblatt, M. *J. Solid State. Chem.* **1990**, *88*, 278.

0897-4756/94/2806-2172$04.50/0

Nd_2NiO_{4+x} showed a semiconductor–metal transition as a function of temperature.[31] Recent results for La_2NiO_{4+x} suggest, however, that the transition may be a consequence of oxygen loss at higher temperatures.[33] Stoichiometric Nd_2NiO_4 is antiferromagnetic (Neel temperature = 320 K). The addition of excess oxygen suppresses the magnetic ordering and no antiferromagnetic transition was observed in oxygen rich samples down to 1.5 K.[26]

Much of the previous work has focused on stoichiometric Nd_2NiO_4 and very little is known about the phase diagram at higher oxygen contents. The previous results on La_2NiO_4[8,9] suggest that an electrochemical determination of the phase diagram at ambient temperature should be possible. In this paper, the feasibility of using electrochemical intercalation to study the Nd_2NiO_{4+x} system at 298 K is evaluated. The composition range where the kinetics are sufficiently rapid to obtain phase relationship from electrochemical measurements has been determined. The phase diagram for Nd_2NiO_{4+x} ($x \leq 0.08$) is reported and the results are compared with data for La_2NiO_{4+x}.

Experimental Section

Nd_2NiO_{4+x} was prepared by dissolving stoichiometric amounts of Nd_2O_3 (Aldrich 99.99%, predried at 700 °C) and NiO (Aldrich, 99.99%) in dilute nitric acid. After the complete dissolution of the oxides, 1 M KOH was added until the pH of the solution was 14.[21] A gelatinous precipitate was formed which was filtered and washed several times with water until the pH of the filtrate was neutral. This precipitate was dried at room temperature and then heated in air at 300 °C for 3 h, 400 °C for 12 h, and 1200 °C for 12 h. The sample was ground after the 400 and 1200 °C heatings. After the final firing the sample was furnace cooled to room temperature.

Electrochemical experiments were performed at 25 °C under nitrogen using a Biologic MacPile potentiostat–galvanostat combination and a three-electrode system. All potentials were measured with respect to a Hg/HgO/1 M KOH (E_0 = +0.098 V vs SCE) reference electrode. The counter electrode was a gold foil of large area. The working electrode consisted of a pellet of the starting material (8 mm diameter, 60 mg) that was sintered at 1325 °C for 12 h and then furnace cooled at room temperature. The pellet was painted on one surface with gold paste and a 0.025 cm diameter platinum wire was attached. The gold film was then dried in air at room temperature and then heated at 900 °C for 12 h. Pellets without gold paint but heat treated in the same way were analyzed thermogravimetrically and iodometrically to determine the oxygen content. The pellet densities were typically ~70% of the theoretical density.

Thermogravimetric analysis was performed on the starting material using a DuPont 951 thermobalance in a 5% hydrogen–95% nitrogen atmosphere to determine the oxygen content. The oxygen content was determined from eight experiments to be 4.17 ± 0.02 by measuring the weight loss on reduction to Nd_2O_3 and nickel metal.

Table 1. X-ray Data for Single-Phase Samples of Nd_2NiO_{4+x} Prepared Electrochemically

$4+x$	a (Å)	b (Å)	c (Å)	strain[a]	ref
4.00	5.382(2)	5.578(2)	12.111(4)	0.0179(4)	*b*
4.04	5.477(2)		12.200(4)		*b*
4.06	5.469(2)		12.199(4)		*b*
4.08	5.462(2)		12.207(1)		*b*
4.18[c]	5.377(2)	5.438(2)	12.337(4)	0.0056(4)	*b*
4.0	5.3876	5.5883	12.135	0.0183	26
4.0	5.3814(2)	5.5850(2)	12.1143(4)	0.0186	27
4.04	5.4487	5.4664	12.206	0.0016	26
4.06[d]	5.465	5.471	12.211	0.0005	22
4.16	5.3775(6)	5.441(1)	12.355(1)	0.0059	24

[a] $(b-a)/(a+b)$. [b] This work. [c] Starting material. [d] Estimated from cell constants.

Modified iodometric titrations were performed on the starting material to determine the oxygen content.[34] A sample of approximately 0.2 mmol was dissolved in ~2 mL of a 4.4 M solution of HBr. The solution was transferred to a flask containing 20 mL of a 0.2 M solution of KI and concentrated NH_4OH was then added to neutralize all but 1 mmol of the acid. The resultant NiI_2 precipitate was then redissolved by addition of 5 mL of a 1 M solution of sodium citrate. The iodine produced was titrated with standard (0.1 M) sodium thiosulfate with starch as the indicator. An oxygen content of 4.17 ± 0.02 was obtained (average of four measurements) for the starting material in good agreement with the thermogravimetric analysis data.

X-ray powder diffraction patterns were obtained using a Scintag XDS2000 diffractometer using Cu Kα radiation in the range $10° \leq 2\theta \leq 70°$. Measurements were made on the starting material and on electrodes. The electrodes were mounted directly on the diffractometer and diffraction patterns were recorded from the front surface. No lines due to NiO were observed in the diffraction pattern of the starting material. Lattice parameters were determined using the GSAS (least-squares refinement) program.[35] The X-ray data were indexed initially with an orthorhombic unit cell corresponding to a supercell ($\sqrt{2}a \times \sqrt{2}a \times c$) of the parent K_2NiF_4 structure and the intensities were fitted in space group *Bmab* (No. 64) with starting parameters taken from ref 26. The compounds with $x = 0.04, 0.06, 0.08$ were found, however, to be very close to tetragonal. Consequently, the data were rerefined with space group *F4/mmm* (No. 139) and only the tetragonal lattice constants are reported in Table 1. It is important to emphasize that this approach is used only to extract values of the lattice constants and does not imply that the detailed structure is properly represented by either space group. Detailed structural models that properly account for octahedral tilts and the distribution of interstitial oxygen atoms are likely to the more complex. The X-ray data are, however, relatively insensitive to the details of the oxygen atom distribution and determining lattice constants by fitting with the *Bmab* and *F4/mmm* models is a good approximation.

The microstructures of the electrodes were examined by scanning electron microscopy using an ISI SS40 instrument. A typical microstructure is shown in Figure 1 for the surface and for a cross section of an electrode. The Nd_2NiO_{4+x} particle size are 5–10 μm.

Results

The powder X-ray diffraction data for the starting material $Nd_2NiO_{4.18}$ along with other single-phase compositions made by electrochemical methods together with some earlier results[22,24,26,27] are shown in Table 1. (The initial composition is taken as the value deter-

(25) Buttrey, D. J.; Harrison, H. R.; Honig, J. M.; Schartman, R. R. *J. Solid State Chem.* **1984**, *54*, 407.
(26) Rodríguez-Carvajal, J.; Fernández-Díaz, M. T.; Martínez, J. L.; Fernández, F.; Saez-Puche, R. *Europhys. Lett.* **1990**, *11*, 261.
(27) Saez-Puche, R.; Fernández, F.; Rodríguez-Caravajal, J.; Martínez, J. L. *Solid State Commun.* **1989**, *72*, 273.
(28) Batlle, X.; Obradors, X.; Martínez, B. *Phys. Rev. B* **1992**, *45*, 2830.
(29) Buttrey, D. J.; Honig, J. M. *J. Solid State Chem.* **72**, *38*, 1988.
(30) Chen, C. H.; Cheong, S.-W.; Werder, D. J.; Takagi, H. *Physica C* **1993**, *206*, 183.
(31) Ganguly, P.; Rao, C. N. R. *Mater. Res. Bull.* **1973**, *8*, 405.
(32) Granados, X.; Fontcuberta, J.; Alonso, J.; Vallet, M.; Gonzalez-Calbet, J. M. *Physica C* **1992**, *191*, 371.
(33) Bassat, J. M.; Odier, P.; Loup, J. P. *J. Solid State Chem.* **1994**, *110*, 124.
(34) Appelman, E. H.; Morss, L. R.; Kini, A. M.; Geiser, U.; Umezawa, A.; Crabtree, G. W.; Carlson, K. D. *Inorg. Chem.* **1987**, *26*, 3237.
(35) Von Dreele, R. B.; Larson, A. C. *GSAS Users Guide*; Los Alamos National Laboratory, Los Alamos, NM 1985–1992.

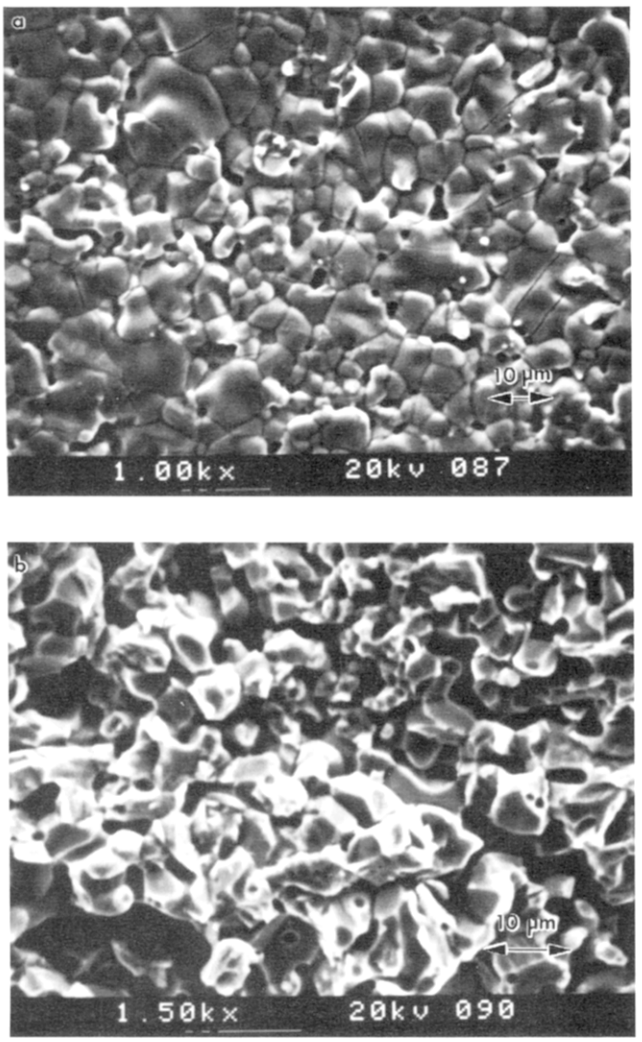

Figure 1. Scanning electron micrographs of (a, top) the top surface and (b, bottom) a cross section of a Nd_2NiO_4 electrode.

mined electrochemically; see below.) The lattice parameters of the starting material $Nd_2NiO_{4.18}$ and the stoichiometric phase, Nd_2NiO_4 are in good agreement with previous reports[26,27] (see Table 1). The phase diagram based on the structural and electrochemical observations will be discussed later.

All the electrochemical experiments were carried out using the potential step method.[36] A more detailed description of the application of this technique to study oxygen intercalation is given in ref 17. In the present experiments, the potential was changed in 5 mV steps and the current decays were recorded. The potential was stepped whenever the current fell below a preset value of 10 μA. The value of the current cutoff determines how close the experiment is to open circuit conditions (equilibrium).

Figure 2 shows the first reduction of the $Nd_2NiO_{4.18}$ starting material. The total degree of reduction indicates an initial oxygen content corresponding to $Nd_2NiO_{4.18}$ (assuming that the final product is $Nd_2NiO_{4.0}$). Previous experience with La_2NiO_{4+x} has shown that compositions below $La_2NiO_{4.0}$ cannot be obtained at voltages above hydrogen evolution. As the limiting composition is approached, the voltage falls off very rapidly with composition. The X-ray diffraction pattern

(36) Thompson, A. H. *J. Electrochem. Soc.* **1979**, *126*, 603.

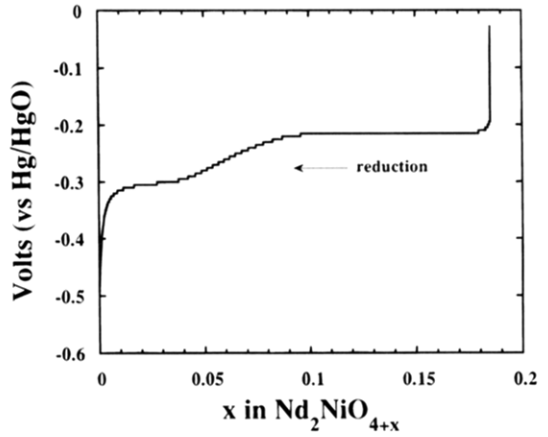

Figure 2. Potential step data for the first reduction of $Nd_2NiO_{4.18}$ in aqueous 1 M KOH. Each voltage step is 5 mV, and the cutoff current is 10 μA.

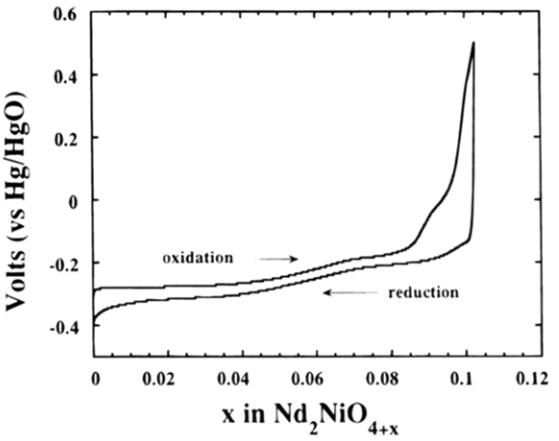

Figure 3. Potential step data for the first oxidation and second reduction of Nd_2NiO_{4+x} showing the reversible region ($0.0 \leq x \leq 0.08$).

of the product at the end of the reduction indicates that the phase formed electrochemically is identical to La_2NiO_4 prepared by hydrogen reduction. A similar situation is observed for Nd_2NiO_4. The lattice constants of the final product are close to the literature values for samples prepared by hydrogen reduction (see Table 1).[26,27] The composition determined from the electrochemical data is in agreement with the thermogravimetric analysis and iodometric titration values, $Nd_2NiO_{4.17\pm0.02}$. The composition determined electrochemically is assumed in the following discussion.

The reduction of $Nd_2NiO_{4.18}$ begins with a long constant-voltage plateau suggesting that a two-phase region exists between $Nd_2NiO_{4.18}$ and $Nd_2NiO_{4.08}$ (Figure 2). The two-phase region is then followed by a single phase from $Nd_2NiO_{4.08}$ to $Nd_2NiO_{4.04}$. In the single-phase region, the voltage at the end of each step varies approximately linearly with composition. Further reduction results in another two phase region between $Nd_2NiO_{4.04}$ and $Nd_2NiO_{4.01}$. Finally a narrow single-phase region is observed between $Nd_2NiO_{4.01}$ and $Nd_2NiO_{4.0}$.

At the end of the first reduction cycle, the sample ($Nd_2NiO_{4.0}$) was electrochemically reoxidized (5 mV steps with a cutoff current of 10μA) in order to determine the reversibility of the intercalation process. The data in Figure 3 show that intercalation of oxygen in Nd_2NiO_{4+x} is only electrochemically reversible in the

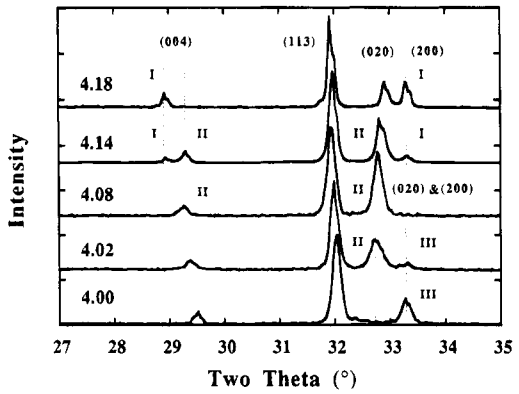

Figure 4. X-ray diffraction data for electrochemically prepared samples of Nd_2NiO_{4+x}. The highest composition phase ($x = 0.18$), the intermediate tetragonal phase and the $x = 0$ composition are labeled I, II, and III, respectively. Dotted lines indicate the evolution of two-phase regions.

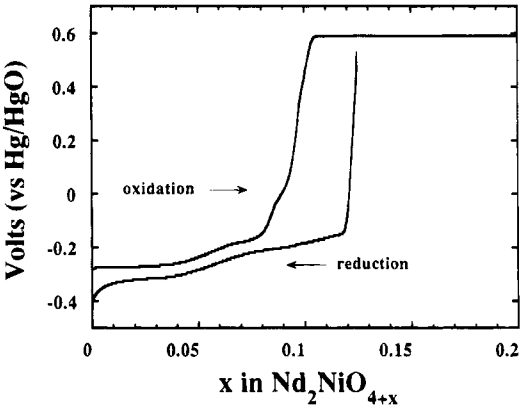

Figure 5. Potential step data for oxidation and reduction of Nd_2NiO_{4+x}. Oxygen evolution occurs on oxidation at ~0.6 V.

range $0 \leq x \leq 0.08$ (the displacement of oxidation and reduction curves is approximately $2iR$, where R is the cell resistance and i the cutoff current). The oxidation is electrochemically irreversible after the composition $Nd_2NiO_{4.08}$ is reached as evidenced by the differences in the oxidation and reduction curves. A maximum value of $Nd_2NiO_{4.10}$ (instead of $Nd_2NiO_{4.18}$) is obtained before the oxygen evolution side reaction occurs. Figure 5 shows the oxidation/reduction behavior of a sample that was left at oxygen evolution for 36 h. On reduction of this sample electrochemically to $Nd_2NiO_{4.0}$, it was found that the oxidized sample had reached a composition $Nd_2NiO_{4.12}$. Oxidation of the sample continues in parallel with oxygen evolution and presumably the starting composition would be recovered in time. Sample oxidation in parallel with oxygen evolution has also been observed for La_2CuO_4.[10]

The general features of the phase behavior were also determined by X-ray diffraction measurements on samples with intermediate oxygen compositions prepared electrochemically. The compositions were chosen to confirm directly the phase diagram inferred from the electrochemical data (Figure 2). Figure 4 and Table 1 show the X-ray diffraction results. At $x = 0.0$, the sample was single phase and the lattice parameters were in good agreement with those previously obtained by Rodríguez-Carvajal et al.[26] At $x = 0.02$, the sample is a two-phase mixture of $Nd_2NiO_{4.0}$ and $Nd_2NiO_{4.04}$. A single-phase region exists for compositions between 0.04 and 0.08, with little change in the lattice parameters. For $x = 0.14$, a two-phase mixture corresponding to $Nd_2NiO_{4.18}$ and $Nd_2NiO_{4.08}$ was observed. Finally, as mentioned above the starting material with $x = 0.18$ was single phase with lattice parameters in good agreement with those previously reported.[24] Thus, the structural data (Table 1 and Figure 4) and the electrochemical results (Figure 2) are consistent and confirm two single-phase regions for $x < 0.01$ and $0.04 \leq x \leq 0.08$ and two miscibility gaps for $0.01 \leq x \leq 0.04$ and $0.08 \leq x \leq 0.18$.

Thermodynamic information was obtained in the single-phase region between $Nd_2NiO_{4.04}$ and $Nd_2NiO_{4.08}$. The relevant formulas and method of calculation were reported elsewhere.[8] An enthalpy of oxidation of −204 kJ/mol of O_2 was estimated for the single-phase region.

Discussion

Oxygen can be intercalated electrochemically at room temperature in Nd_2NiO_{4+x} from aqueous 1 M KOH. On the first reduction cycle, all of the excess oxygen is removed resulting in the formation of $Nd_2NiO_{4.0}$. The lattice constants of the electrochemically prepared $Nd_2NiO_{4.0}$ agree with results obtained for samples prepared by hydrogen reduction. The changes in voltage with composition on reoxidation closely follow the reduction data as far as $x = 0.08$. A two-phase region, $0.01 \leq x \leq 0.04$, is followed by a single-phase extending to $x = 0.08$. The orthorhombic strain in the Nd_2NiO_4 structure is substantially reduced on insertion of interstitial oxygen at all compositions and is zero in the composition range $0.04 \leq x \leq 0.08$. Further oxidation to compositions greater than $x = 0.08$ is irreversible. The rapid increase in voltage to the value where oxygen evolution occurs (Figure 3) indicates a substantial kinetic barrier to the reformation of the initial composition, $Nd_2NiO_{4.18}$. An X-ray diffraction pattern of a sample left at oxygen evolution for 36 h (Figure 4) indicated the formation of a small amount of a second phase which qualitatively appeared to be $Nd_2NiO_{4.18}$ together with a majority phase of $Nd_2NiO_{4.08}$. The orthorhombic strain increases on reoxidation of $Nd_2NiO_{4.08}$ back to the starting material, but in view of the reversibility at lower composition where the strain also changes, it seems unlikely that this alone is responsible for the kinetic barrier. The reoxidation data also show an inflection in the voltage curve at $x \approx 0.09$, suggesting the possibility of an intermediate phase between $Nd_2NiO_{4.08}$ and $Nd_2NiO_{4.12}$. In contrast, the initial reduction results in Figure 1 suggest that no intermediate phases exist for $0.08 \leq x \leq 0.18$. More detailed studies and experiments at higher temperature are required to resolve this point.

The general intercalation behavior of Nd_2NiO_4 is similar to that reported previously for $La_2NiO_{4.145}$[8,9] but with detailed differences in the range of compositions over which oxygen atoms can be intercalated and deintercalated reversibly and in the maximum composition that can be obtained below oxygen evolution ($x \leq 0.14$, La_2NiO_4; and $x \leq 0.1$, Nd_2NiO_4). A comparison of electrochemical potential step reduction data for Nd_2NiO_{4+x} and La_2NiO_{4+x} ($0.00 \leq x \leq 0.10$) is shown in Figure 6. The data have the same voltage steps and cutoff currents. The sample sizes and therefore current densities are also similar. The reduction of Nd_2NiO_{4+x} occurs at more negative potentials in comparison to La_2NiO_{4+x}. The more negative potentials indicate that oxygen atom removal (reduction) is more difficult for

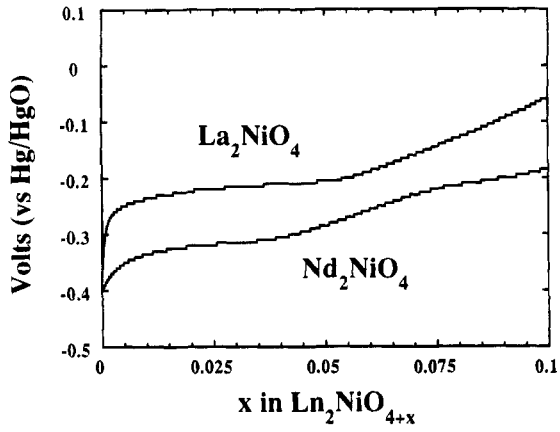

Figure 6. Comparison of the composition dependence of the reduction potentials of La_2NiO_{4+x} and Nd_2NiO_{4+x} in the range $0 \leq x \leq 0.10$.

Nd_2NiO_{4+x}. Because the mechanisms for oxygen intercalation are presumably similar in both materials, the difference in potentials is due to the effect of structural differences on the thermodynamics. The difference between the two compounds is opposite to that which is normally observed in perovskite oxides where generally decreasing the size of the A cation decreases the stability of the higher oxidation state transition-metal ion. The distortion from the ideal K_2NiF_4 tetragonal structure in Nd_2NiO_4, however, is greater than in La_2NiO_4. Consequently, removal of excess oxygen atoms from Nd_2NiO_{4+x} increases the structural strain and is apparently less energetically favorable than the corresponding process in La_2NiO_{4+x}. Oxygen removal from Nd_2NiO_{4+x}, therefore, occurs at lower potentials than from La_2NiO_{4+x}.

The electrochemical data for both La_2NiO_4 and Nd_2NiO_4 are similar but significantly different from the reported behavior of La_2CuO_4. The electrochemical behavior of La_2CuO_4 at comparable reaction rates shows that the oxidation and reduction processes are much further from equilibrium than in the nickel systems. The difference is consistent with the lower value of the diffusion coefficient reported for the copper system.[37] Further studies of electrochemistry, structure and physical properties of the 214 compounds, in single-crystal form, are currently in progress to determine diffusion coefficients and provide more detailed phase diagrams.

Acknowledgment. We thank D. J. Buttrey for helpful discussions. The work was supported in part by the Robert A. Welch foundation (Grant No. 1207) and by the National Science Foundation (CHE-9408742).

(37) Grenier, J.-C.; Wattiaux, A.; Pouchard, M. In *Phase Separation in Cuprate Superconductors*, Muller, K. A.; Benedek, G., Eds.; World Scientific: Singapore, 1993; pp 187–207.